Supporting information

Multifunctional Zinc Oxide Promotes Electrochemiluminescence of Porphyrin Aggregates for Ultrasensitive Detection of Copper Ion

Qian Han[†,‡], Cun Wang[†,§], Zhuozhe Li[†], Jingling Wu[†], Pingkun Liu[†], Fangjing Mo[†], Yingzi Fu*[†]

[†]*Key Laboratory of Luminescent and Real-Time Analytical Chemistry (Southwest University), Ministry of Education, School of Chemistry and Chemical Engineering, Southwest University, Chongqing 400715, China*

[‡]*Laboratory of Environment Change and Ecological Construction of Hebei Province, College of Resources and Environment Science, Hebei Normal University, Shijiazhuang, Hebei 050024, China*

[§]*Chongqing Collaborative Innovation Center for Functional Food, Chongqing University of Education, Chongqing 400067, China*

Corresponding author: Yingzi Fu

Tel: +86-023-68252277

E-mail address: fyzc@swu.edu.cn

Table of Contents

1. Reagents and Material

5,10,15,20-tetrakis(4-carboxyphenyl)porphyrin (TCPP) and L-cysteine (L-Cys) were purchased from Sigma-Aldrich, zinc acetate dihydrate ($Zn(CH_3COO)_2 \cdot 2H_2O$), citric acid, sodium dodecyl sulfate (SDS), cetyltrimethylammonium bromide (CTAB) and potassium persulfate ($K_2S_2O_8$, 99.99%) were gained from Aladdin Biochemical Technology Co., Ltd (Shanghai, China). Sodium hydroxide (NaOH) and hydrochloric acid (HCl) were obtained from the Chemical Reagent Co. (Chongqing, China). 0.1 $mol \cdot L^{-1}$ Phosphate buffer solutions (PBS) at various pH values were prepared by mixing the different ratio stock solutions of KH_2PO_4 and Na_2HPO_4 which containing 0.1 $mol \cdot L^{-1}$ KCl. 5.0 m $mol \cdot L^{-1}$ $[Fe(CN)_6]^{4-/3-}$ (pH 7.4) solution was prepared with $K_4Fe(CN)_6$ and $K_3Fe(CN)_6$ containing 0.1 $mol \cdot L^{-1}$ KCl. All chemicals were analytical grade and used as received without further purification. Ultrapure water was used through the whole experiments (Millipore, 18.2 MΩ·cm).

2. Apparatus and Characterization

The morphologies of the TCPP aggregates and ZnO@Cys NFs were obtained using a JEM-2100 field emission scanning electron microscopy (SEM) equipped with a field emission gun at 200 kV on JEOL-7800F, an energy-dispersive X-ray spectroscopy (EDS, INCA X-Max 250, Japan). The X-ray photoelectron spectroscopy (XPS) analysis was examined under a VG Scientific ESCALAB 250 spectrometer (Thermoelectricity Instruments, USA). The UV-Vis and photoluminescence (PL) spectra measurements were carried out on a UV-2600 UV/vis spectrophotometer (Shimadzu, Japan) and a fluorescence spectrometer (Shimadzu, F-7000 PC, Japan),

respectively. The PL lifetime spectra were measured by a Florolog-3 Fluorescence Spectrometer (Horiba). A Jasco J-815 circular dichroism (CD) spectrometer (Tokyo, Japan) was employed for CD spectral measurements of ZnO@Cys NFs.

The ECL measurements were performed on a model MPI-E electrocheminescence analyzer (Xi'an Ramax Electronicscience Technology Co. Ltd., Xi'an, China) with the voltage of the photomultiplier tube (PMT) setting at 750 V, the potential scanning from 0 – -1.5 V and the scan rate of 200 $mV \cdot s^{-1}$ in the process of detection. A three-electrode system was used in the experiment with bare and the modified glassy carbon electrode (GCEs, Φ = 4 mm) as the working electrode, an Ag/AgCl reference electrode and a Pt wire counter electrode, respectively. Cyclic voltammetry (CV) and electrochemical impedance spectroscopy (EIS) measurements were conducted at a CHI 604 D electrochemistry workstation (Shanghai Chenhua Instruments Co, China) in 5.0 $mmol \cdot L^{-1}$ $[Fe(CN)_6]^{3-/4-}$ solution (pH 7.4). All measurements were carried out at the room temperature of 25 ± 1°C.

3. Electrochemical behaviors of the different modified electrodes

The stepwise fabrication process of the proposed sensor was recorded by cyclic voltammetry (CV) and electrochemical impedance spectroscopy (EIS) in 5.0 mmol·L^{-1} $[Fe(CN)_6]^{3-/4-}$ solution (pH 7.4).[1] The corresponding CV curves were shown in Figure S1 A, and a well-defined redox peak was obtained on the bare GCE (curve a). Owing to the weak electrical conductivity of TCPP aggregates, a decrease of redox peak was appeared on TCPP aggregates/GCE (curve b). The redox peak decreased clearly as the doping of ZnO@Cys NFs onto the TCPP aggregates surface (ZnO@Cys NFs/TCPP aggregates/GCE), owing to the electric barrier of ZnO@Cys NFs (curve c). Figure S1B showed impedance curves of the stepwise modification process. The Ret corresponded to the semicircle diameter, which indicated the restricted diffusion of the substance modified in the surface of GCE. The bare GCE showed an almost straight line (curve a). After ZnO@Cys NFs (curve c) and TCPP aggregates (curve b) were sequentially modified onto the electrode, however, the value of Ret increased continually.

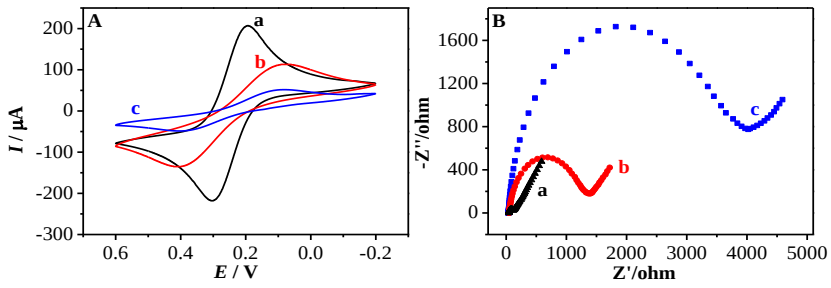

Figure S1. (A) CV and (B) EIS responses in 5 mmol·L^{-1} $[Fe(CN)_6]^{3-/4-}$ solution of different electrodes: (a) bare GCE, (b) TCPP aggregates/GCE, (c) ZnO@Cys NFs/TCPP aggregates/GCE

4. Elemental mapping images of TCPP aggregates

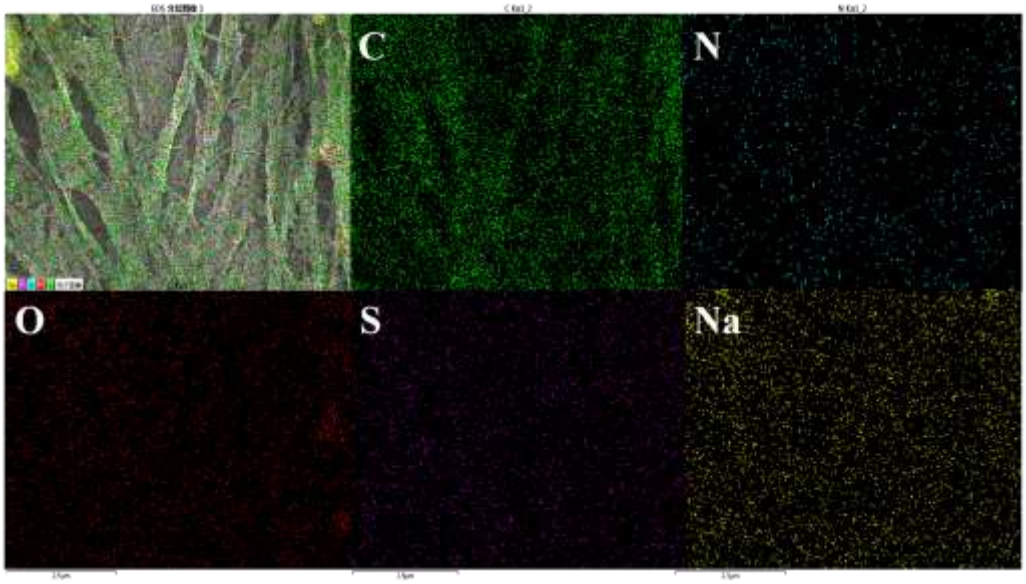

Figure S2. Elemental mapping images of TCPP aggregates and related elements C, N, O, S, Na.

5. Elemental mapping images of ZnO@Cys NFs

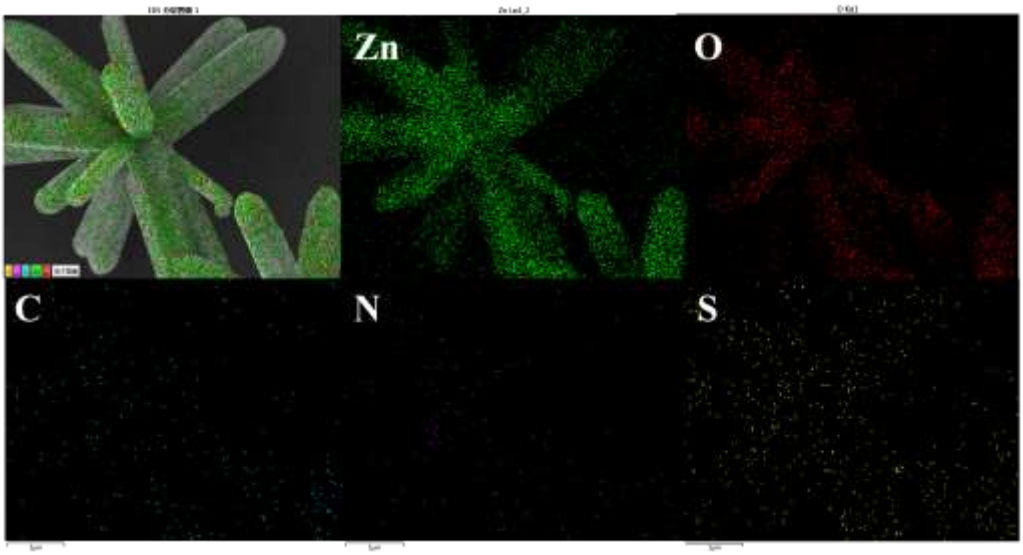

Figure S3. Elemental mapping images of ZnO@Cys NFs, and related elements Zn, O, C, N, S.

6. The EIS and CV curves of coreactant and coreactant accelerator

We further investigated the reaction between the coreactant accelerator (ZnO@Cys NFs) and the coreactant ($S_2O_8^{2-}$) via electrochemical impedance spectroscopy (EIS) and cyclic voltammetry (CV) system. Compared with bare GCE in 0.05 mol·L^{-1} $S_2O_8^{2-}$ solution, ZnO@Cys NFs/GCE in 0.05 mol·L^{-1} $S_2O_8^{2-}$ solution shows a small semicircle, implying significant improvement on the electron transfer rate (Figure S4A, bare GCE as the control). As shown in Figure S4B, the bare GCE was measured in 0.05 mol·L^{-1} $S_2O_8^{2-}$ solution (curve a), a reduction peak at -1.09 V and a pair of weak redox peaks at 0.16 V and −0.12 V of $S_2O_8^{2-}$ were observed, which was assigned to the reduction of $S_2O_8^{2-}$.[2] While an apparently reduction peak shifted positively from -1.09 V to -0.975 V on ZnO@Cys NFs/GCE (curve b), and the peak currents increases distinctly in comparison with that of $S_2O_8^{2-}$ solution, indicating the ZnO@Cys NFs can improve the electron transfer of $S_2O_8^{2-}$.[3,4] All results showed that ZnO@Cys NFs as a coreactant accelerator promote the reduction of $S_2O_8^{2-}$ to generate more intermediate radical ($SO_4^{\bullet-}$).

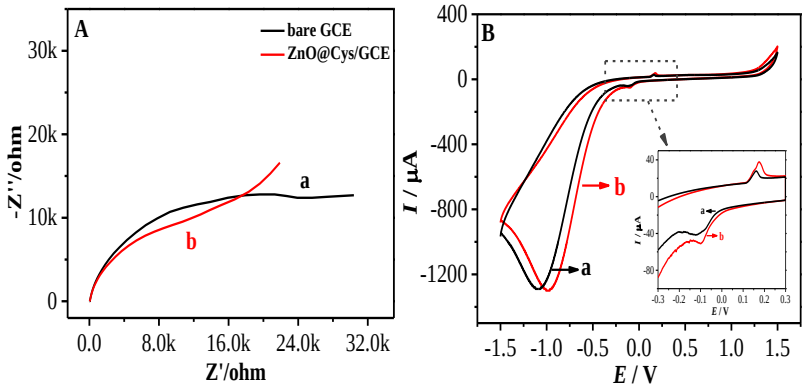

Figure S4. (A) EIS and (B) CV curves of bare GCE (curve a), ZnO@Cys NFs/GCE (curve b) in 0.1 mol·L^{-1} PBS (pH 7.4) containing 0.05 mol·L^{-1} $S_2O_8^{2-}$; inset B: the

amplification of curves a and b.

7. The ECL efficiency of TCPP aggregates and TCPP mononer

The ECL efficiency was calculated through the following relation.[5]

$$\Phi_{ECL} = \left(\frac{\int \mathrm{ECL}\,\mathrm{d}t}{\int \mathrm{Current}\,\mathrm{d}t} \right)_x \Big/ \left(\frac{\int \mathrm{ECL}\,\mathrm{d}t}{\int \mathrm{Current}\,\mathrm{d}t} \right)_{st} \times 100\%$$

where “ECL” and “Current” represent ECL intensities and electrochemical current values, respectively, “st” refers to the $Ru(bpy)_3Cl_2/K_2S_2O_8$ standard and “*x*” refers to the TCPP aggregates (or TCPP monomer) analyte.

8. SEM image and UV-vis of other TCPP aggregates

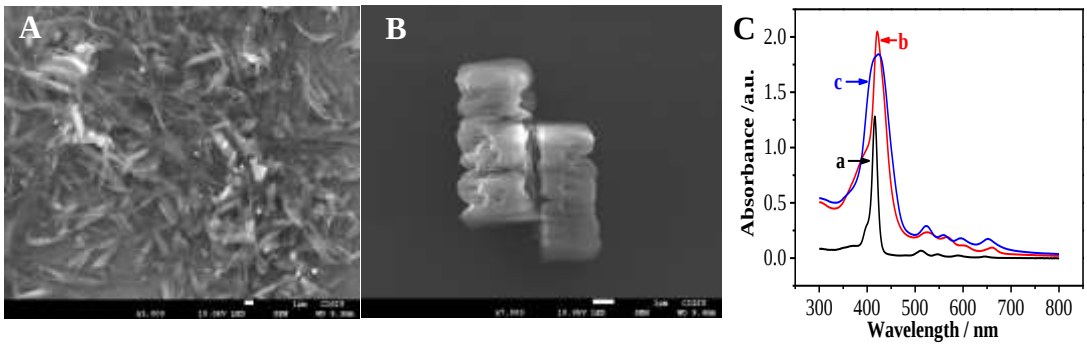

Figure S5. SEM images of (A) CTAB-assisted TCPP aggregates and (B) TCPP aggregates without SDS. (C) UV-vis spectra of (a) TCPP monomer, (b) CTAB-assisted TCPP aggregates and (c) TCPP aggregates without SDS.

9. Optimization of the Experimental Conditions

In order to achieve the best sensing performance, the ECL working conditions were optimized. The effect of solution pHs (5.0-8.5) on the ECL intensities were tested (Figure S6A). When the pH values are from 7.0 to 7.5, the ECL intensities increase with increasing pH until reaching an approximate plateau. With the further increase the pH, the ECL intensity goes down. The too low pH would inhibit the electro-reduction of TCPP, while the intermediate $SO_4^{\bullet-}$ of $S_2O_8^{2-}$ would be consumedat too high pH. Considering the practical application and strongest ECL intensity observed at pH 7.4, the pH 7.4 is chosen as the optimum pH.

Also, the amount of ZnO@Cys NFs directly affects the stability and ECL intensity of TCPP aggregates modified electrode. Figure S6B depicts the ECL intensities change with different volumes of ZnO@Cys NFs ($1mg \cdot mL^{-1}$). The most stable and

best ECL response are achieved at 5 μL of ZnO@Cys NFs. Considering the practical application and strongest ECL intensity, the 5 μL ZnO@Cys NFs are chosen in the further experiments.

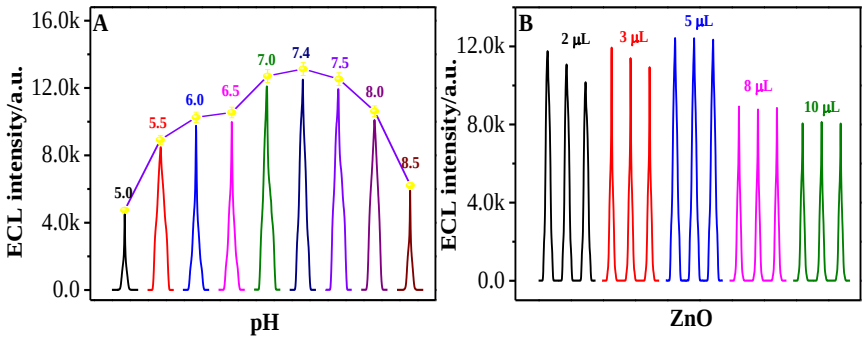

Figure S6. The optimization of experimental parameters: (A) Effect of the pH. (B) The influence of different volumes of ZnO@Cys NFs.

10. Recovery experiment

Table S1 Recovery Tests for Cu^{2+} in Tap Water (n = 6)

Samples	Added (nm)	Founded (nm)	Recovery（%）	RSD(%, n=6)
1	0.100	0.0986	98.6	3.4
2	0.500	0.515	103	2.2
3	1.00	0.99	99	1.5
4	10.0	10.3	103	2.8
5	100	102	102	3.1

References

(1) Jiang, M. H.; Li, S. K.; Zhong, X.; Liang, W. B.; Chai, Y. Q.; Zhuo, Y. and Yuan, R. *Anal. Chem.* **2019**, *91*, 3710-3716.

(2) Zhou, Y.; Chen, M. X.; Zhuo, Y.; Chai Y. Q.; Xu, W. J.; and Yuan, R. *Anal. Chem.* **2017**, *89*, 6787−6793.

(3) Zhang, X. L.; Li, W. M.; Zhou, Y.; Chai Y. Q.; and Yuan, R. *Biosens. Bioelectron.* **2019**, *135*, 8-13.

(4) Lei, Y. M.; Xiao, B. Q.; Liang, W. B.; Chai, Y. Q.; Yuan, R.; Zhuo, Y. *Biosens. Bioelectron.* **2018**, *109*, 109-115.

(5) Zhang, R. Z.; Adsetts, J. R.; Nie,Y. T.; Sun, X. H.; Ding, Z. F. *Carbon* 2**018**, *129*, 45-53.